University of Glasgow
DEPARTMENT OF
AEROSPACE
ENGINEERING

omputation of Turbulent Pitching Aerofoil Flows

K.J. Badcock

Aero Report 9322

September 14, 1993

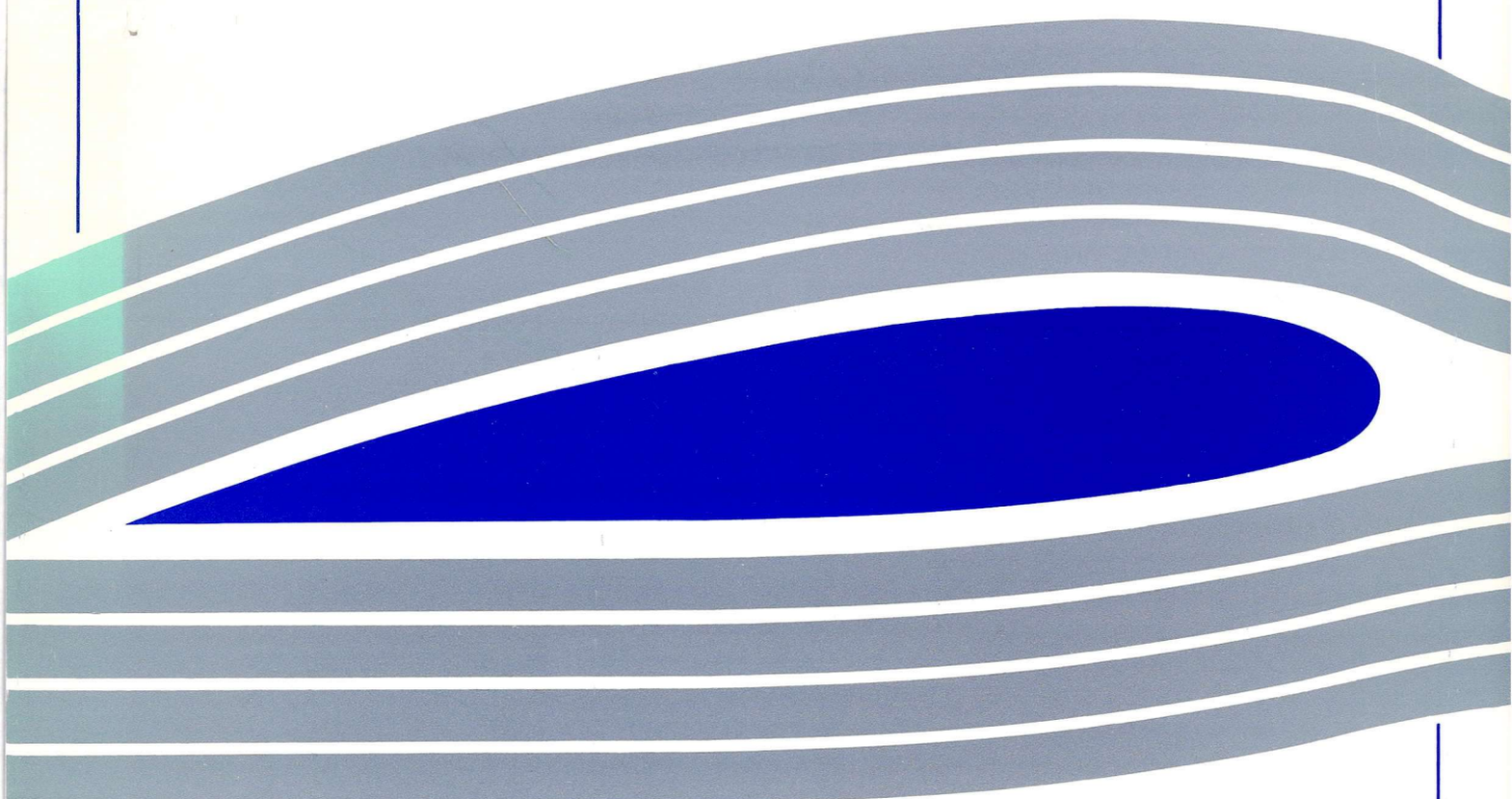

Computation of Turbulent Pitching Aerofoil Flows

K.J. Badcock

Aero Report 9322

September 14, 1993

Computation of Turbulent Pitching Aerofoil Flows

K.J. Badcock *
Aerospace Engineering Department
University of Glasgow,
Glasgow, G12 8QQ, U.K.
EMAIL:gnaa36@uk.ac.glasgow.udcf

September 14, 1993

Abstract

An unfactored implicit method for the unsteady, turbulent Navier-Stokes equations is adapted for pitching aerofoil flows. The mesh is moved rigidly with the aerofoil. Parameter tests on the method are presented. Test cases examined are from the AGARD aeroelastic configurations and involve the NACA0012 and NACA64A010 aerofoils. Detailed comparisons with experiment are presented.

*This work was carried out under SERC contract.

Contents

1 Introduction

An important part of the design process for aircraft is the demonstration that the flight envelope lies outside regions of aeroelastic instability. Due to the cost of aeroelastic wind tunnel experiments, computational tools should have an important role to play in this area. However, simulation techniques for unsteady flow lag well behind the development of codes for steady flows where convergence acceleration by multigrid, Newton iterations or a variety of other methods has reached an advanced stage where studies of three dimensional flows governed by the Navier-Stokes equations are being reported in the literature with increasing frequency.

The basis of most aeroelastic and many unsteady aerodynamic studies has been the the low frequency transonic small disturbance equations. The code LTRAN, developed by Ballhaus and Goorjian, which uses an Alternating Direction Implicit approach to solve the equation in multi dimensions provided a major breakthrough in computational aerodynamics. Adaptions to the code have included the addition of high frequency terms and a coupling with boundary layer codes to account for viscous effects leading to off-shoots such as XTRAN from the US airforce and ATRAN from NASA Ames research centre. Extensive studies using these codes have been published including the aeroelastic response of aerofoils in 1978 [1], the three-dimensional flow around rigid [2] and flexible [3] wings in 1982, the extensive flutter analysis of F-5 [4] and B-1 [5] wings in 1985 and 1986 respectively and for the aeroelastic response of a complete F-16C aircraft in 1988 [6].

One of the principal disadvantages of a code like LTRAN is its inability to cope with strong shockwaves. To model this flow feature satisfactorally the lowest level of model required is the Euler equations. Magnus and Yoshihara published a solution of the Euler equations in 1976. As computational methods have matured and computing facilities improved it has become more common to solve the unsteady Euler equations. During the 1980's significant efforts have been published by the research teams of Lerat, Whitfield and Jameson. In 1991 results were published for the unsteady flow around a rigid rectangular wing [7] as part of the development process for the NASA Ames code ENSAERO. Three-dimensional aeroelastic results were obtained by the NASA Langley code CFL3D in 1991. Both of these codes use a Beam-Warming approximate factorisation. An unfactored method was used in [8] to yield results for rigid LANN and NORA wings and in [9] for an F-5 wing.

The Navier-Stokes equations have remained relatively untouched for unsteady applications despite the need to model fully separated and mixed

separated-attached flows. Notable unsteady Navier-Stokes calculations include the study of Aileron Buzz [10] published by Steger and Bailey, Levy et al [11] [12] who studied shock induced oscillations over a rigid aerofoil and Chyu et al [13] who examined the flow over a pitching NACA64A010 aerofoil, a flow that has become a standard test case for Euler and Navier-Stokes codes. From 1990 Guruswamy and co-workers have reported results obtained with the three-dimensional Euler/Navier-Stokes code ENSAERO [14] [15] [16] [7] [17]. Applications include the aeroelastic flow over F-5 and delta wings. In 1990 an application of the Lockheed code ENS3D was reported to examine the flutter response of a wing-fuselage section. These studies are mostly based on the Beam-Warming approximate factorisation method which utilises central differences and artificial dissipation although there is an indication that upwind methods are becoming increasingly popular.

During the 1980's significant advances were made in algorithms for the Euler and Navier-Stokes equations and for the solution of linear algebraic systems. The development of upwind schemes of the flux-vector splitting or approximate Riemann solver type for the Euler equations led to very satisfactory ways of treating shockwaves and had the additional benefit that when some of these methods were incorporated in Navier-Stokes codes, boundary layers could be well resolved due to their low numerical dissipation.

A crucial element of some steady and most unsteady CFD codes is the efficient solution of a large sparse linear system. This is usually achieved by some form of approximate factorisation which introduces an additional source of error into the solution procedure with consequences for accuracy and efficiency. However, the Alternating Direction Implicit method has proved very popular and successful with its incorporation in the Beam-Warming algorithm and in codes such as LTRAN and ARC3D. More recently an approximate LU factorisation which is based on a flux vector splitting has been successfully used. Conjugate gradient methods provide an efficient method for solving the exact linear system to a required tolerance and they have been used successfully for steady problems. The preconditioning strategy is crucial to their success and in [18] the ADI factorisation was used to provide a preconditioner. This method, called AF-CGS (Approximate Factorisation Conjugate Gradient Squared), proved successful on a number of rigid test problems.

It is clear from reported aeroelastic studies that efficient Navier-Stokes codes are required for many applications. Due to the intensive computing required by such codes efficient numerical algorithms together with improved computing power are required for the use of Navier-Stokes codes

for three-dimensional geometries to become routine. In the present paper the development of an unfactored method based on upwind methods and conjugate gradient solvers is continued. We present comparisons with experimental data for the AFCGS code applied to pitching aerofoil flows. The test cases are selected from the AGARD standard aeroelastic configurations.

In the following section a brief description of the AFCGS method is given. For the full details the reader is referred to [18]. Results are then presented for five AGARD test cases for the NACA0012 and NACA64A010 aerofoils.

2 AF-CGS Method

The thin-layer Navier-Stokes equations in generalised co-ordinates are given by

$$\frac{\partial \mathbf{w}}{\partial t} + \frac{\partial \mathbf{f}}{\partial \xi} + \frac{\partial \mathbf{g}}{\partial \eta} = (Re)^{-1} \frac{\partial \mathbf{s}}{\partial \xi} \tag{1}$$

where

$$\mathbf{w} = J^{-1} \begin{bmatrix} \rho \\ \rho u \\ \rho v \\ e \end{bmatrix}, \mathbf{f} = J^{-1} \begin{bmatrix} \rho U \\ \rho u U + \xi_x p \\ \rho v U + \xi_y p \\ U(e+p) - \xi_t p \end{bmatrix}, \mathbf{g} = J^{-1} \begin{bmatrix} \rho V \\ \rho u V + \eta_x p \\ \rho v V + \eta_y p \\ V(e+p) - \eta_t p \end{bmatrix}$$

$$\mathbf{s} = J^{-1} \begin{bmatrix} 0 \\ \mu m_1 u_\xi + (\mu/3) m_2 \xi_x \\ \mu m_1 v_\xi + (\mu/3) m_2 \xi_y \\ \mu m_1 m_3 + (\mu/3) m_2 (\xi_x u + \xi_y v) \end{bmatrix}.$$

Here,

$$U = \xi_t + \xi_x u + \xi_x v$$

$$V = \eta_t + \eta_x u + \eta_x v$$

$$m_1 = \xi_x^2 + \xi_y^2$$

$$m_2 = \eta_x^2 + \eta_y^2$$

$$m_3 = (u^2 + v^2)/2 + Pr^{-1}(\gamma - 1)^{-1}(c^2)_\xi$$

and J is the determinant of the Jacobian of the transformation $x = x(\xi, \eta, t)$ and $y = y(\xi, \eta, t)$. Here ρ, u, v, e, p, Pr, Re, c, γ denote density, the two components of velocity, energy, pressure, the Prandtl number, the Reynolds number, the speed of sound and the constant ratio of the specific heats respectively. The viscosity is composed of a part due to the natural viscosity of the fluid and a term to account for turbulence. Sutherland's law is used to describe the variation of the fluid viscosity with temperature.

The Baldwin-Lomax model is used to provide a value for the turbulent viscosity. Since none of the flows examined herein involve massive separation no modification of the turbulence model is used.

To solve this system of partial differential equations a finite volume scheme is used which has various features. For the spatial terms Osher's method is used. For general geometries the details of Osher's method are described in [19]. A MUSCL interpolation is used to provide second or third order accuracy and the Von Albada limiter prevents spurious oscillations from occuring around shock waves. Central differencing is employed for the viscous terms. Far-field boundary conditions are imposed by Riemann-invariants and no vortex correction is applied due to the unsteadyness of the flow.

The temporal discretisation is based on the backward Euler method. An efficient mixed analytic and finite difference procedure is used to generate the required Jacobian of the spatial discretisation. The linear system obtained is solved by the conjugate gradient squared (CGS) method with the alternating direction implicit approximate factorisation providing a preconditioner. The reader is refered to [18] for full details.

The problems we consider herein relate to pitching aerofoils. Since no deformation of the aerofoils is considered the mesh can be rotated rigidly with the aerofoil. Defining the starting mesh points by $\{x = x_0\}_{i,j}$, $\{y = y_0\}_{i,j}$ the transformed mesh at time t_1 is given by

$$\{x = r_0 cos(\alpha(t_1) - \alpha_0) + l(1 - cos(\alpha_0))\}_{i,j}$$

$$\{y = r_0 sin(\alpha(t_1) - \alpha_0) + l sin(\alpha_0)\}_{i,j}$$

where the aerofoil pitches about the point $(l,0)$, the initial incidence is α_0 and $r^2_{0_{i,j}} = x^2_{0_{i,j}} + y^2_{0_{i,j}}$. The mesh velocities can be easily evaluated given an analytical form for α. No-slip boundary conditions on the aerofoil can then be imposed.

3 AF-CGS parameter tests

In this section we shall examine the AF-CGS method applied to moving aerofoil flows with regard to optimising the number of time steps per cycle of the motion and the tolerance of the CGS solution. The choice of the time step is determined by a balance between minimising the number of steps whilst retaining a well-preconditioned linear system for the conjugate gradient solution. The other point of interest is the effect on the accuracy of the choice of time step and also of the CGS tolerance which should be chosen to be large enough to yield a stable method without compromising accuracy.

To test these points experimental runs were carried out for an AGARD pitching aerofoil test case (case 5 in table 1 below) for various combinations of the parameters. The same mesh was used for each case. First, to examine the effect on accuracy of the time step and the CGS-tolerance the pressure distribution is plotted in figure 1 at one time for three cases involving 150 and 500 time steps per cycle and tolerances of 10^{-1} and 10^{-2}. It can be seen that the distributions for each of the conditions are identical and so it is concluded that the solution arising from 150 steps per cycle and a tolerance of 10^{-1} is a good one on this mesh.

Secondly, the CPU time to compute three non-dimensional time units of the flow on a SUN SPARCstation10 was noted for varying time steps and tolerances for the AF-CGS method and these are compared in figure 2 with the time required by ADI which proved unstable for up to 700 steps per cycle. There is a clear minimum for the AF-CGS curves indicating the balance in chosing the time step which was discussed above. It is clear that for larger time steps there is a significant saving in CPU time by using a higher tolerance for the CGS solution. For smaller time steps the CGS iteration frequently converges after only one step and so the setting of a higher tolerance becomes redundant.

From the results presented in this section it is clear that 100-200 steps per cycle and a tolerance of 10^{-1} yields the most efficient method without compromising accuracy.

A brief mesh refinement study was carried out to verify that the solution obtained on a 70 by 32 mesh is adequate. The comparison with a solution obtained on a 128 by 40 mesh is shown in figure 3. The solution on the finer mesh has a better resolved shock wave but apart from this there is little difference between the sets of results and hence it is concluded that the coarser grid gives reasonably converged results.

4 AGARD Test Cases

The AGARD sub-committee on aeroelasticity defined test cases to act as standard flows for computer code evaluation and verification. In this paper we present results for several of these test cases for pitching aerofoils. The motion is defined by the angle of attack as a function of time and the centre of rotation x_c which is given herein as a distance along the chord as a percentage of the chord length. The angle of attack is defined as

$$\alpha(\tau) = \alpha_m + \alpha_0 sin(k\tau) \tag{2}$$

where $\tau = tl/V_{\text{inf}}$ is the non-dimensional time.

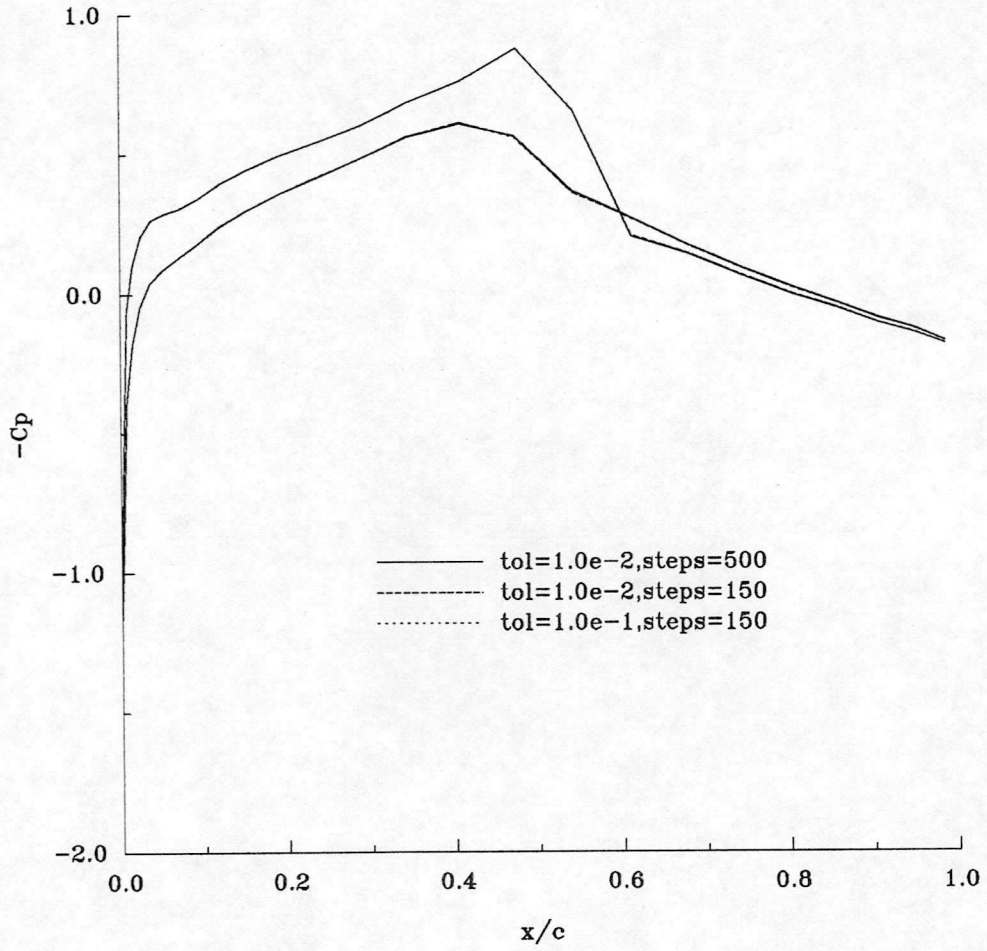

Figure 1: *Effect of CGS tolerance and time step on the pressure distribution for AGARD NACA64A010 ct6.*

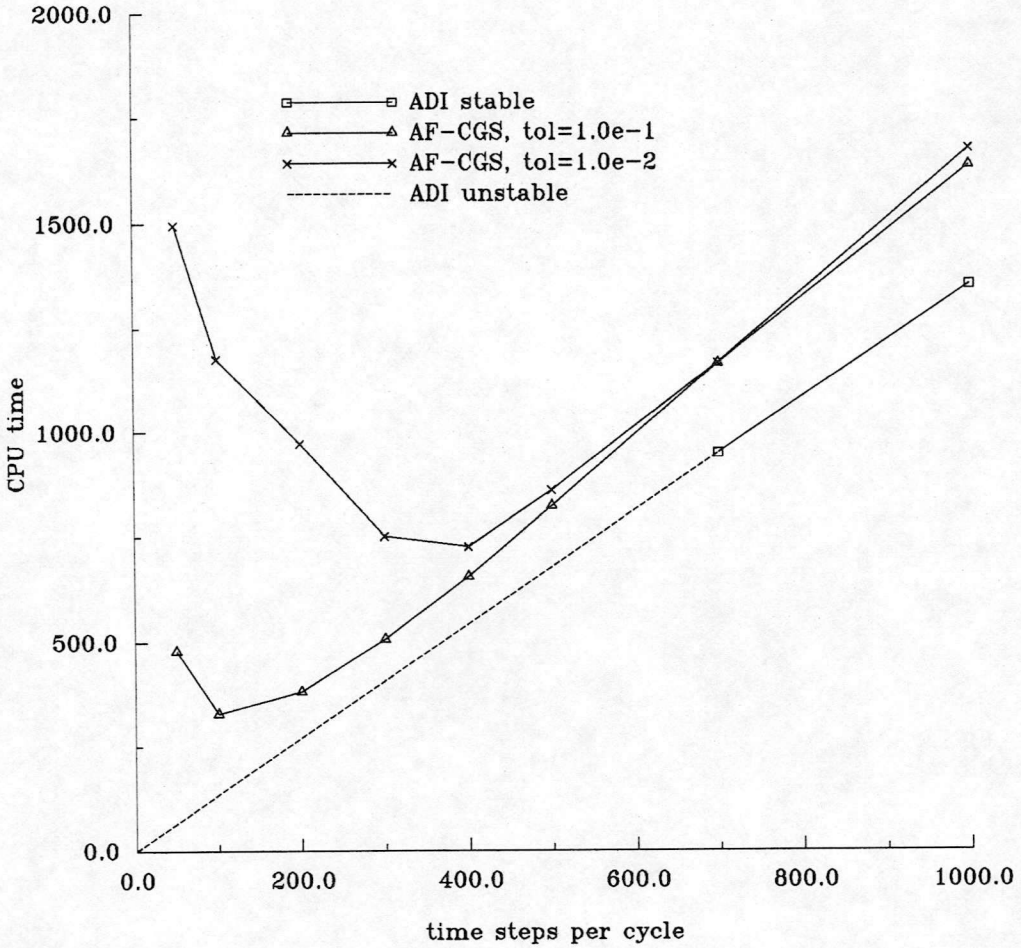

Figure 2: *CPU time required to compute three non-dimensional time units on a SPARCstation 10 for the AF-CGS and ADI methods. The dotted line indicates that ADI is unstable at these time steps.*

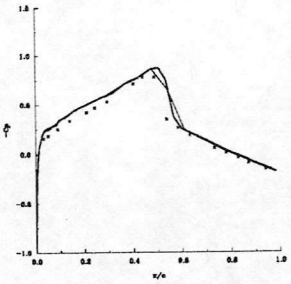

$\alpha = 1.00^o$

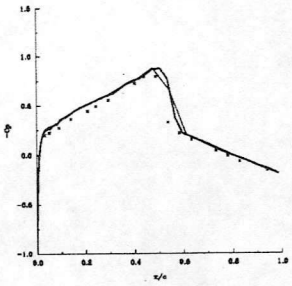

$\alpha = 0.74^o$

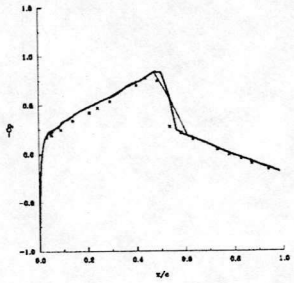

$\alpha = -1.06^o$

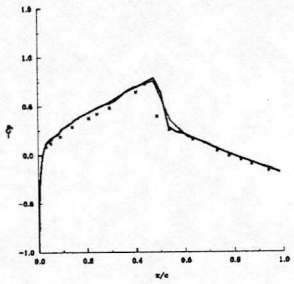

$\alpha = -0.73^o$

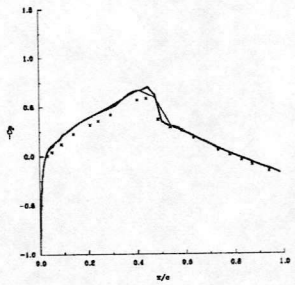

$\alpha = -1.01^o$

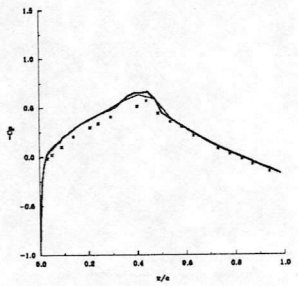

$\alpha = -0.59^o$

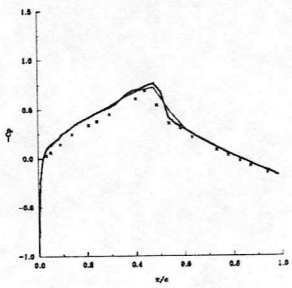

$\alpha = 0.21^o$

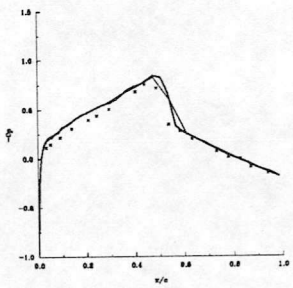

$\alpha = 0.87^o$

Figure 3: $-C_p$ vs x/c for case 5. x-experiment, solid line - mesh 70 by 32, dashed line 128 by 40

number	aerofoil	M_{inf}	$Re \times 10^6$	α_m	α_0	k	x_c
1	NACA0012	0.60	4.8	2.89	2.41	0.1616	0.25
2	NACA0012	0.60	4.8	3.16	4.59	0.1622	0.25
3	NACA0012	0.60	4.8	4.86	2.44	0.1620	0.25
4	NACA0012	0.755	5.5	0.016	2.51	0.1628	0.25
5	NACA64A010	0.796	12.56	0.	1.0	0.204	0.248

Table 1: *Test cases examined in this paper.*

The cases considered, which are listed in table 1, are selected because detailed pressure distributions are available at a number of points during the cycle. All of the results are obtained on a 71 by 33 C-mesh which was generated by the Eagle grid generation package. The far field is located at 10 chords. The AFCGS method is used throughout with the CGS tolerance set at 10^{-1}. The number of time steps per cycle for each case is 150. Detailed comparisons for all the cases are shown for the pressure distributions at eight separate times during one cycle. Data for case 5 was only available for the upper surface. The results are discussed in section 5.

Cases 1-5 represent attached flows. Several computational studies of these cases have been published. Transonic small-disturbance results were presented in [20] for case 5. Full potential results for case 5 were given in [21] and detailed pressure distribution comparisons for case 1 in [22] where excellent agreement was achieved. The Euler equations were solved in [23] for case 1, in [9] for case 5 and in [24] for cases 1,4 and 5. Detailed pressure comparisons were made in each case and improved shock resolution is notable over the full potential results. Finally, Euler and Navier-Stokes results were presented in [25] for case 4 from which it was suggested that the mean corrected experimental angle of attack for this case should be higher. All of the results reported show good agreement with experiment because the shock strength is weak enough for the full potential equations and there is no large scale separation for the Euler equations. Hence these test cases should not represent a serious challenge for a Navier-Stokes code but it is important to establish that the code can indeed deal with these cases since aeroelastic applications to aerofoils are based on these flows. It is also interesting to evaluate the efficiency of the unfactored time-stepping approach. Further tests are required to establish the ability of the code, and especially the turbulence model, to deal with large scale separation.

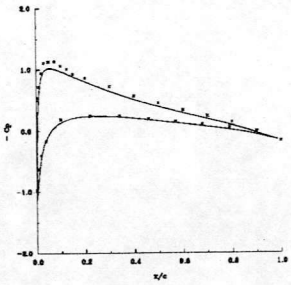

$\alpha = 2.97^o$

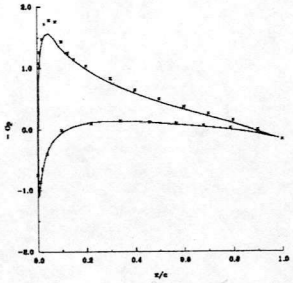

$\alpha = 4.56^o$

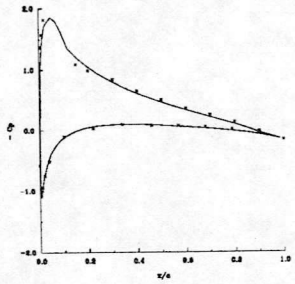

$\alpha = 5.09^o$

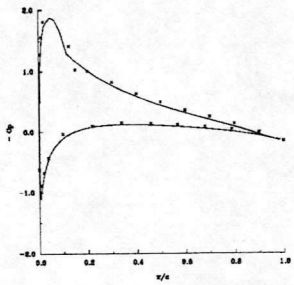

$\alpha = 4.17^o$

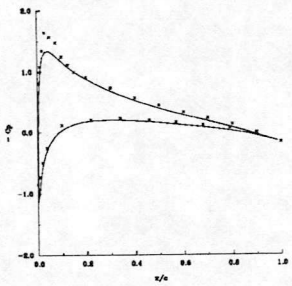

$\alpha = 2.62^o$

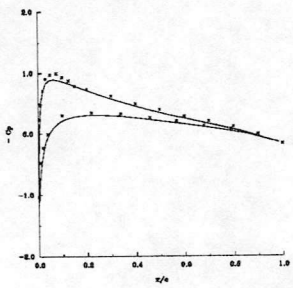

$\alpha = 1.16^o$

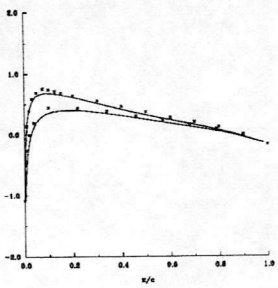

$\alpha = 0.48^o$

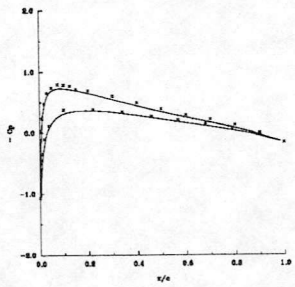

$\alpha = 1.29^o$

Figure 4: $-C_p$ *vs* x/c *for case 1. x-experiment, line- computed*

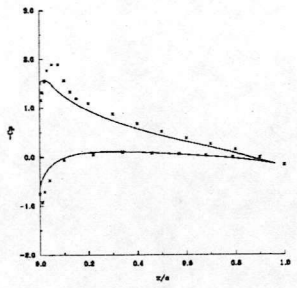

$\alpha = 5.32^o$

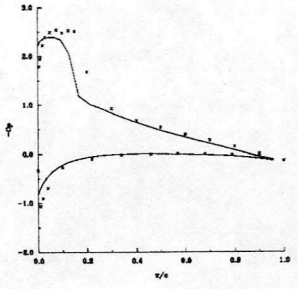

$\alpha = 7.36^o$

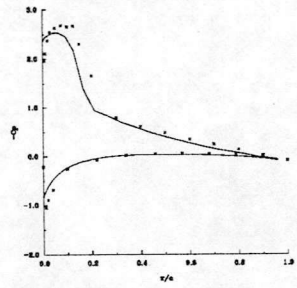

$\alpha = 6.80^o$

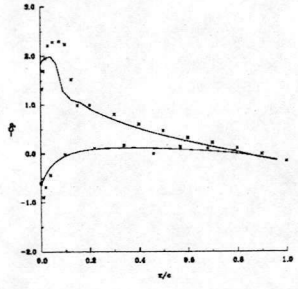

$\alpha = 3.88^o$

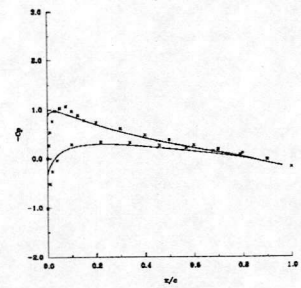

$\alpha = 0.86^o$

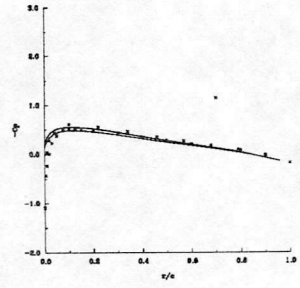

$\alpha = -1.30^o$

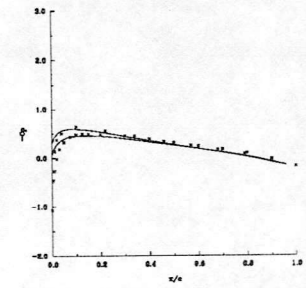

$\alpha = -0.57^o$

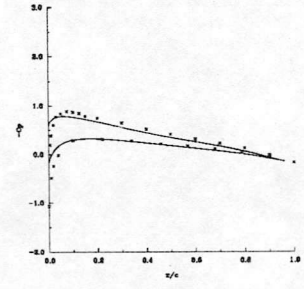

$\alpha = 2.38^o$

Figure 5: $-C_p$ vs x/c case 2. x-experiment, line - computed

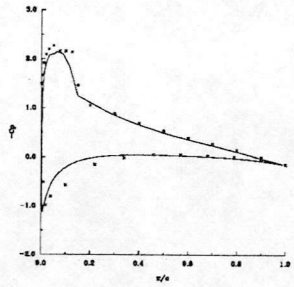

$\alpha = 5.94^o$

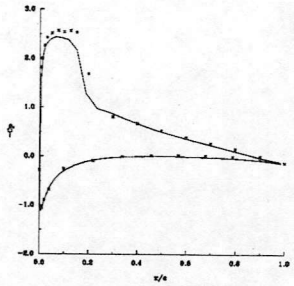

$\alpha = 6.96^o$

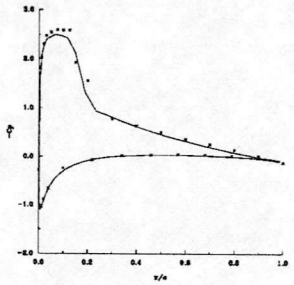

$\alpha = 6.59^o$

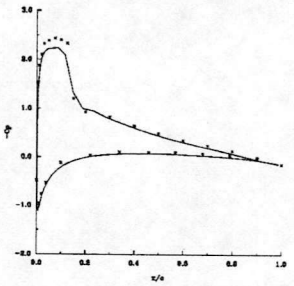

$\alpha = 5.12^o$

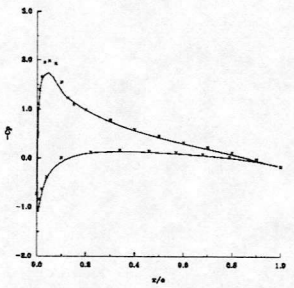

$\alpha = 3.51^o$

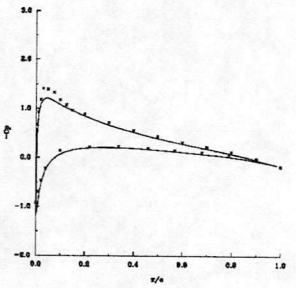

$\alpha = 2.44^o$

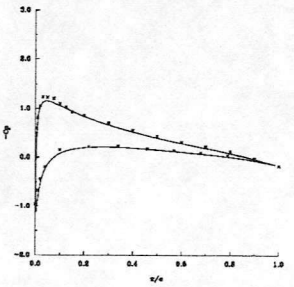

$\alpha = 2.67^o$

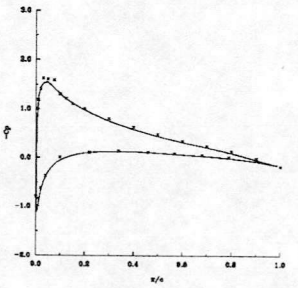

$\alpha = 4.27^o$

Figure 6: $-C_p$ vs x/c for case 3. x-experiment, line - computed

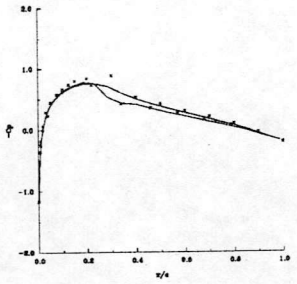

$\alpha = 1.07^o$

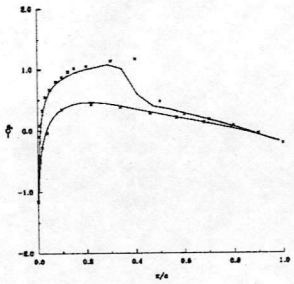

$\alpha = 2.34^o$

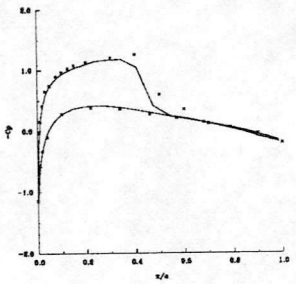

$\alpha = 2.02^o$

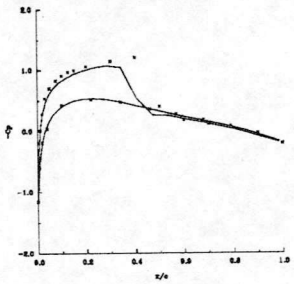

$\alpha = 0.53^o$

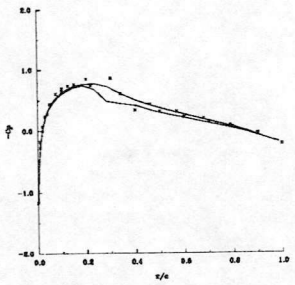

$\alpha = -1.24^o$

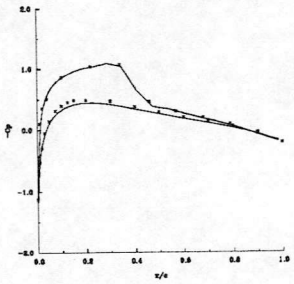

$\alpha = -2.41^o$

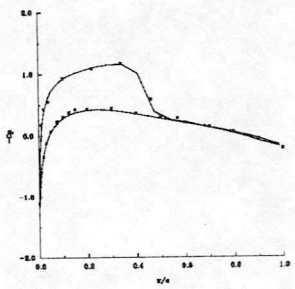

$\alpha = -2.01^o$

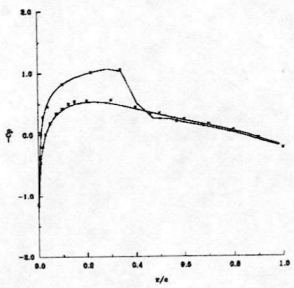

$\alpha = -0.56^o$

Figure 7: $-C_p$ vs x/c for case 4. x-experiment, line - computed

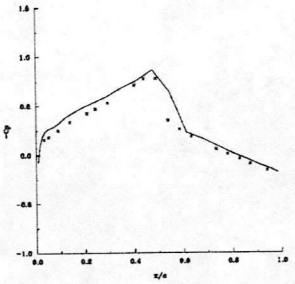

$\alpha = 1.00^o$

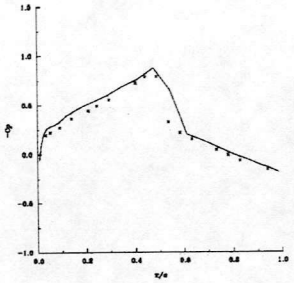

$\alpha = 0.74^o$

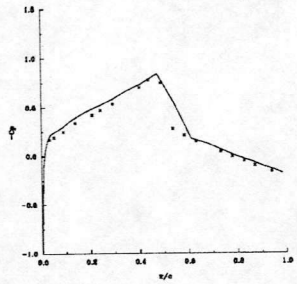

$\alpha = -1.06^o$

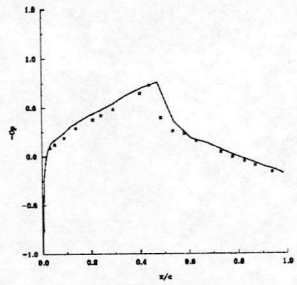

$\alpha = -0.73^o$

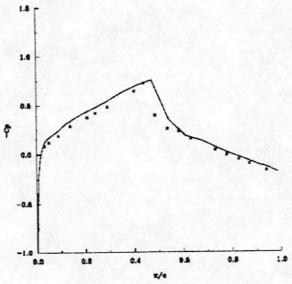

$\alpha = -1.01^o$

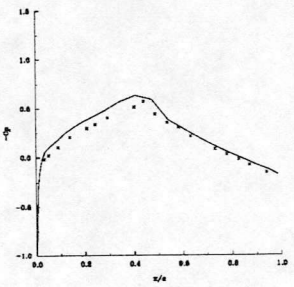

$\alpha = -0.59^o$

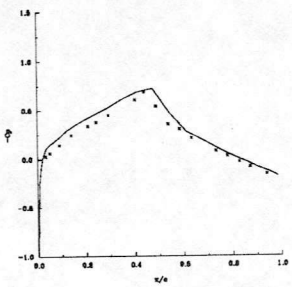

$\alpha = 0.21^o$

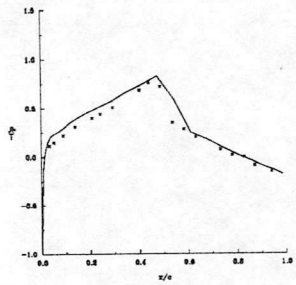

$\alpha = 0.87^o$

Figure 8: $-C_p$ vs x/c for case 5. x-experiment, line - computed

5 Discussion

The detailed pressure distribution comparisons are shown in figures 4- 8. In general good agreement with the experimental data of [26] is noted.

For case 1 the position and strength of the shock which forms on the upward part of the motion[1] is well predicted. There is some diagreement with experiment at the leading edge during the downward part of the cycle. The shock resolution is slightly worse than for the Euler results of [23] and [24] but this can be ascribed to the coarser grid used in the present work. The comparison away from the shock is in closer agreement with experiment than the Euler solutions.

The AF-CGS code has some difficulty in locating the shockwave during the upward part of the motion for case 2 with the shock being predicted upstream of the experimental position.

Case 3 is well predicted with excellent resolution of the shockwave. Small discrepancies aorund the leading edge during the downward part of the motion are again noted.

The shock location for case 4 during the upward part of the motion is slightly upsteam of experiment but is in close agreement during the downward part of the motion as for case 2. This is consistent with the results in [25] where the discrepancies are attributed to wall effects. Almost identical pressure distributions to those in [25] are achieved on a much coarser grid in the present study.

Good agreement with experiment is achieved for case 5. The results are very similar to the Euler solution of [24] confirming that no significant viscous effects are present for this flow.

6 Conclusions

An efficient unfactored fully implicit method has been tested for standard AGARD pitching aerofoil flows. It was found that the method was stable for a time step which is 4-5 times bigger than an approximately factored algorithm. This increases the efficiency of the present method by a factor of four over the approximate factorisation method with the additional advantage of increased robustness.

The method was verified for several test cases involving pitching NACA0012 and NACA64A010 aerofoils. Excellent agreement was noted with both experiment and previous computations which were all performed on finer meshes. These cases represent attached flow and so are not in general rep-

[1] In this section the aerofoil motion is described in terms of the movement of the nose i.e. the upward motion denotes the case where α is increasing.

resentative of the flow problems which need to be studied by solving the Navier-Stokes equations. However, it is anticipated that the main problem in dealing with separated flow would be with the turbulence model and not with the solution algorithm.

References

[1] W.F. Ballhaus and P.M. Goorjian. Computation of unsteady transonic flows by the indicial method. *AIAA J.*, 16:117–124, 1978.

[2] D.P.Rizzetta C.J. Borland and H. Yoshihara. Numerical solution of three-dimensional unsteady transonic flow over swept wings. *AIAA J.*, 20:340–347, 1982.

[3] D.P.Rizzetta C.J. Borland and H. Yoshihara. Nonlinear transonic flutter analysis. *AIAA J.*, 20:1606–1615, 1982.

[4] P. Guruswamy and P.M. Goorjian. Efficient algorithm for unsteady transonic aerodynamics of low-aspect-ratio wings. *AIAA J.*, 22:193–199, 1985.

[5] H. Ide G.P. Guruswamy, P.M. Goorjian and G.D. Miller. Transonic aeroelastic analysis of the B-1 Wing. *J. Aircraft*, 23:547–553, 1986.

[6] D.A. Seidel H.J. Cunningham J.T. Batina, R.M. Bennett and S.R. Bland. Recent advances in transonic computational aeroelasticity. *Computers and Structures*, 30:29–37, 1988.

[7] G.P. Guruswamy. Unsteady aerodynamic and aeroelastic calculations for wings using Euler equations. *AIAA J.*, 28:461–469, 1990.

[8] A. Brenneis and A. Eberle. Evaluation of an unsteady implicit Euler code against two and three-dimensional standard configurations. In *Transonic Unsteady Aerodynamics and Aeroelasticity*. AGARD, 1991.

[9] A. Brenneis and A. Eberle. Application of an implicit relaxation method solving the Euler equations for time-accurate unsteady problems. *J. Fluids Eng.*, 112:510–520, 1990.

[10] J.L. Steger and H.E. Bailey. Calculation of transonic aileron buzz. *AIAA J.*, 18:249–255, 1980.

[11] L.L. Levy. Experimental and computational steady and unsteady transonic flows about a thick airfoil. *AIAA J.*, 16:564–572, 1978.

[12] L.L. Levy J.B. McDevitt and G.S. Deiwert. Transonic flow about a thick circular-arc airfoil. *AIAA J.*, 14:606–613, 1976.

[13] K.S. Chang W.J. Chyu, S.S. Davis. Calculation of unsteady transonic flow over an airfoil. *AIAA J.*, 19:684–690, 1981.

[14] N.M. Chadrejian and G.P. Guruswamy. Transonic Navier-stokes computations for an oscillating wing using zonal grids. *AIAA J.*, 29:326–335, 1992.

[15] G.P. Guruswamy. Navier-Stokes computations on swept-tapered wings,including flexibility. *J. Aircraft*, 29:588–597, 1992.

[16] G.P. Guruswamy S. Obayashi and P.M. Goojian. Streamwise upwind algorithm for computing unsteady transonic flows past oscillating wings. *AIAA J.*, 29:1668–1677, 1991.

[17] G.P. Guruswamy and S. Obayashi. Transonic aeroelastic computations on wings using Navier-Stokes equations. In *Transonic Unsteady Aerodynamics and Aeroelasticity*. AGARD, 1991.

[18] K.J.Badcock. An efficient unfactored implicit method for unsteady aerofoil flows. Technical report, G.U. Aero report 9313, 1993.

[19] S.Osher and S.R.Chakravarthy. Upwind schemes and boundary conditions with applications to Euler equations in general coordinates. *J. Comp. Phys.*, 50:447–481, 1983.

[20] K.A. Hessenius and P.M. Goorjian. Validation of LTRAN2-HI by comparison with unsteady experiment. *AIAA J.*, 20:731–732, 1982.

[21] J.B Malone and N.L. Sankar. Numerical simulation of two-dimensional unsteady transonic flows using full-potential equation. *AIAA J.*, 22:1035–1041, 1984.

[22] J. Gorski V. Shankar, H. Ide and S. Osher. A fast, time-accurate, unsteady full potential scheme. *AIAA J*, 25:230–238, 1987.

[23] V. Venkatakrishnan and A. Jameson. Computation of unsteady transonic flows by the solution of the Euler equations. *AIAA J.*, 26:974–981, 1988.

[24] A.L. Gaitonde and S.P. Fiddes. A moving mesh system for the calculation of unsteady flows. Technical report, A.I.A.A. 93-0641, 1993.

[25] M.P. Thomadakis and S. Tsangaris. On the prediction of transonic unsteady flows using second order time accuracy. In *Computational Fluid Dynamics '92*, 1992.

[26] J.J. Olsen. Compendium of unsteady aerodynamic measurements. Technical Report 702, AGARD, 1982.